

# Deep Learning-Based Computer Vision Framework for Predicting Retroreflectivity of Road Signs

## Final Report

by

**Denis Ruganuza**  
**Methusela Sulle**  
**Paul Omulokoli**

**Judith L. Mwakalonge, Ph.D.**  
South Carolina State University  
E-mail: [jmwakalo@scsu.edu](mailto:jmwakalo@scsu.edu)

**Gurcan Comert, Ph.D.**  
North Carolina A&T State University  
E-mail: [gcomert@ncat.edu](mailto:gcomert@ncat.edu)

**Saidi Siuhi, Ph.D.**  
South Carolina State University  
E-mail: [ssiuhi@scsu.edu](mailto:ssiuhi@scsu.edu)

**September 2024**



**Center for Connected Multimodal Mobility (C²M²)**



*200 Lowry Hall, Clemson University  
Clemson, SC 29634*

**DISCLAIMER**

*The contents of this report reflect the views of the authors, who are responsible for the facts and the accuracy of the information presented herein. This document is disseminated in the interest of information exchange. The report is funded, partially or entirely, by the Center for Connected Multimodal Mobility (C<sup>2</sup>M<sup>2</sup>) (Tier 1 University Transportation Center) Grant, which is headquartered at Clemson University, Clemson, South Carolina, USA, from the U.S. Department of Transportation's University Transportation Centers Program. However, the U.S. Government assumes no liability for the contents or use thereof.*

*Non-exclusive rights are retained by the U.S. DOT.*

### ACKNOWLEDGMENT

*This research project is sponsored by the US-Department of Transportation (USDOT) through Center for Connected Multimodal Mobility (C<sup>2</sup>M<sup>2</sup>) Tier 1 University Transportation Center (UTC). The transportation Program of South Carolina State University has administrated the research works.*

## TECHNICAL REPORT DOCUMENTATION PAGE

<b>1. Report No.</b>	<b>2. Government Accession No.</b>	<b>3. Recipient's Catalog No.</b>	
<b>4. Title and Subtitle</b> Deep Learning-Based Computer Vision Framework for Predicting Retroreflectivity of Road Signs		<b>5. Report Date</b> September 2024	
		<b>6. Performing Organization Code</b>	
<b>7. Author(s)</b> Denis Ruganuza; ORCID 0009-0005-7701-6072 Methuselah Sulle; ORCID 0000-0002-3240-6019 Paul Olukoye; ORCID 0009-0004-9840-0930 Judith Mwakalonge, Ph.D.; ORCID 0000-0002-7497-6829 Gurcan Comert, Ph.D.; ORCID: 0000-0002-2373-5013 Saidi Siuhi, Ph.D.; ORCID: 0000-0001-8409-9287		<b>8. Performing Organization Report No.</b>	
<b>9. Performing Organization Name and Address</b> South Carolina State University, 300 College Street NE Orangeburg, SC 29115		<b>10. Work Unit No.</b>	
		<b>11. Contract or Grant No.</b> 1918-211-2021810	
<b>12. Sponsoring Agency Name and Address</b> Center for Connected Multimodal Mobility (C2M2) Clemson University 200 Lowry Hall, Clemson Clemson, SC 29634		<b>13. Type of Report and Period Covered</b> Final Report July 2024	
		<b>14. Sponsoring Agency Code</b>	
<b>15. Supplementary Notes</b>			
<b>16. Abstract</b> <p>The retro-reflectivity of traffic signs is essential for road safety, particularly in low-light and adverse weather conditions, by ensuring signs remain visible and legible to road users. However, retro-reflective quality degrades over time due to environmental exposure, reducing sign effectiveness and increasing risks of road accidents and potential liabilities for road agencies. Accurate estimation of traffic signs' lifespan is thus critical for efficient maintenance and resource allocation. While prior studies have analyzed factors affecting retro-reflectivity, such as sign age, color, orientation, and weather, few have utilized deep learning models with expanded input variables.</p> <p>In this study, we address these gaps by examining additional environmental factors, air temperature, relative humidity, and sign age through a deep learning model incorporating image detection. The results of the XGBoost classification model achieved an overall accuracy of 0.97, correctly predicting 97% of instances, while our transfer learning model, EfficientNet-B0 results yielded an R<sup>2</sup> value of 0.79, indicating that 79% of retro-reflectivity variance was explained, highlighting the model's capability to identify signs that fall below retro-reflectivity standards. The model's performance highlights the potential for automating the detection of road signs below required retro-reflectivity standards, reducing maintenance costs, and enhancing road safety through predictive monitoring.</p>			
<b>17. Keywords</b> Deep learning, Transportation Safety, Traffic signs, Retroreflectivity		<b>18. Distribution Statement</b> This report or any part of this report is restricted to published until prior permission from the authors.	
<b>19. Security Classif. (of this report)</b> Unclassified	<b>20. Security Classif. (of this page)</b> Unclassified	<b>21. No. of Pages</b> 25	<b>22. Price</b> NA

## TABLE OF CONTENTS

<b>EXECUTIVE SUMMARY .....</b>	<b>1</b>
<b>CHAPTER 1 .....</b>	<b>2</b>
<b>Introduction.....</b>	<b>2</b>
Objectives of the Project.....	3
<b>CHAPTER 2 .....</b>	<b>4</b>
<b>Literature Review .....</b>	<b>4</b>
Key Factors Affecting Retro-reflectivity .....	4
Advancements in Predictive Modeling .....	4
Comparative Performance of Models .....	4
Challenges and Gaps .....	5
<b>CHAPTER 3 .....</b>	<b>6</b>
<b>Method .....</b>	<b>6</b>
Study area and Data collection. ....	6
Qualitative Analysis of the Data .....	10
Retro-Reflection Degradation Prediction Models .....	11
<b>CHAPTER 4 .....</b>	<b>13</b>
<b>Experimental Setup .....</b>	<b>13</b>
Experimental Setup .....	13
Hyper-parameter Tuning.....	13
Evaluation Metrics .....	14
<b>CHAPTER 5 .....</b>	<b>16</b>
<b>Results and Discussion.....</b>	<b>16</b>
Results and Discussion .....	16
<b>CHAPTER 6 .....</b>	<b>17</b>
<b>Conclusion and Future Work .....</b>	<b>17</b>
Conclusion and Future Work .....	17
<b>REFERENCES.....</b>	<b>18</b>

## List of Tables

Table 1: XGBoost Hyper-parameter Settings. ....	13
---	----

## List of Figures

Figure 1: Workflow diagram showing the integration of retro-reflectivity coefficients, environmental factors, and sign attributes into a dataset, followed by data cleaning, model development, and retro-reflectivity prediction. ....	6
Figure 2: Traffic signs in Orangeburg County, South Carolina, documented as part of the study and obtained from the South Carolina Department of Transportation (SCDOT).....	7
Figure 3: The handheld RetroSign GRX 554 retroreflectometer, used for measuring traffic sign retro-reflectivity during the study (TAPCO, 2024). ....	8
Figure 4: Calibration of the RetroSign GRX 554 retroreflectometer, demonstrating the attachment of the calibration standard and preparation for accurate retro-reflectivity measurements. ....	8
Figure 5: Shows measuring and recording the retroreflectivity coefficient of the Legend color of a stop sign in the study area.....	9
Figure 6: Some of the Images of road signs collected using a retro-reflectometer in the study area. ....	9
Figure 7: Correlation analysis in collected data.....	10

## EXECUTIVE SUMMARY

The retro-reflectivity of traffic signs is essential for road safety, particularly in low-light and adverse weather conditions, by ensuring signs remain visible and legible to road users. However, retro-reflective quality degrades over time due to environmental exposure, reducing sign effectiveness and increasing risks of road accidents and potential liabilities for road agencies. Accurate estimation of traffic signs' lifespan is thus critical for efficient maintenance and resource allocation. While prior studies have analyzed factors affecting retro-reflectivity, such as sign's age, color, orientation, and weather, few have utilized deep-learning models with expanded input variables. We address these gaps by examining additional environmental factors, air temperature, relative humidity, and sign's age through a deep learning model incorporating image detection. Data collection involved a hand-held reflectometer to capture retro-reflective readings alongside sign images and weather data in Orangeburg County, South Carolina, USA. The results of the XGBoost classification model achieved an overall accuracy of 0.97, correctly predicting 97% of instances, while our transfer learning model, EfficientNet-B0 results yielded an  $R^2$  value of 0.79, indicating that 79% of retro-reflectivity variance was explained, highlighting the model's capability to identify signs that fall below retro-reflectivity standards. The model's performance highlights the potential for automating the detection of road signs below required retro-reflectivity standards, reducing maintenance costs, and enhancing road safety through predictive monitoring.

## CHAPTER 1

### Introduction

Traffic signs play a critical role in ensuring roadway safety and order, functioning as visual aids to regulate, warn, and guide road users, thereby supporting traffic flow (Jamal et al., 2022a; Khalilikhah & Heaslip, 2016; Saleh & Fleyeh, 2024a). These signs help reduce driver stress and the likelihood of poor judgment through the provision of clear and actionable information (Ansari et al., 2022). To maintain effectiveness, traffic signs must be detectable, legible, and comprehensible day and night, achieved through specific design attributes like size, color, and text style (Saleh & Fleyeh, 2021), (Jamal et al., 2022a). Key to nighttime visibility is retro-reflectivity, a property in certain materials with tiny glass beads that reflect light back toward its source, enhancing visibility in low-light or adverse weather conditions. While retro-reflectivity is essential for nighttime visibility, its gradual degradation over time reduces visibility and increases the potential for road safety risks, particularly under low-light conditions (Jamal et al., 2022a).

The degradation of retro-reflectivity, particularly at night, has significant implications for road safety, as reduced visibility correlates with higher crash rates. Studies show that nighttime crashes result in higher fatality rates than daytime incidents, with declining retro-reflectivity diminishing the conspicuity and legibility of traffic signs (Brimley et al., 2017). According to the Fatality Analysis Reporting System (FARS), a disproportionate number of road fatalities occur at night, contributing to an estimated 1.19 million annual traffic-related deaths worldwide. Despite its critical importance, most studies have focused on intrinsic factors such as age and physical properties of traffic signs while neglecting the potential role of environmental variables, such as air temperature, humidity, and pollution, in exacerbating retro-reflectivity degradation. These gaps in the literature underscore the urgency of addressing traffic sign degradation as a crucial step in improving road safety and reducing accident rates.

This study builds on prior research by introducing innovative deep learning and computer vision techniques to address retro-reflectivity degradation in traffic signs. Unlike traditional approaches, which often exclude environmental factors, this study incorporates variables such as air temperature, humidity, and pollution into a predictive framework. By integrating these factors with sign attributes like age and shading conditions, the proposed model curates a combined image and tabular retro-reflectivity dataset, enhancing prediction accuracy and addressing data limitations. The study's framework aims to forecast retro-reflectivity values, classify signs as compliant or non-compliant, and facilitate efficient maintenance scheduling, ultimately supporting Manual on Uniform Traffic Control Devices (MUTCD) compliance and enhancing road safety.

## Objectives of the Project

---

This study aims to develop a comprehensive framework to improve the accuracy and robustness of retro-reflectivity degradation predictions for traffic signs, addressing key identified challenges. The framework integrates newly curated image and tabular datasets, incorporates environmental variability, and unifies diverse sign attributes and aging conditions into a single predictive model. By adopting a multi-source data approach, it provides a holistic and adaptable solution for retro-reflectivity forecasting, enhancing maintenance planning and compliance with MUTCD standards. The framework's contributions are as follows

- Develop a robust predictive framework by curating a combined image and tabular retro-reflectivity dataset to address data limitations and enhance model accuracy through visual validation.
- Incorporate environmental factors alongside diverse sign attributes; age and shading conditions, to improve the adaptability of retro-reflectivity predictions.
- Design and implement models to accurately forecast retro-reflectivity values and classify signs as compliant or not enabling efficient maintenance and MUTCD compliance

## CHAPTER 2

### Literature Review

Retro-reflectivity degradation is a critical concern in road safety as it determines the visibility of traffic signage. Accurate prediction of retro-reflectivity loss aids in maintenance scheduling and resource allocation, ensuring consistent road safety. This review explores the key factors influencing retro-reflectivity degradation and evaluates the evolution of predictive methods, emphasizing the transition from traditional regression models to advanced machine learning approaches.

#### Key Factors Affecting Retro-reflectivity

---

Several factors significantly impact retro-reflectivity degradation, with age consistently identified as the most critical. (Wolshon et al., 2022) emphasized the roles of signage orientation and distance from the road, while Roxan Saleh, 2021 highlighted geographic location, climatic conditions, type, age, color, and sunlight exposure as dominant factors. In contrast, factors such as orientation relative to the sun, pollution, and proximity to the roadside were found to have negligible effects. These findings collectively underline the importance of periodic assessments and age-specific maintenance schedules to ensure compliance with retro-reflectivity standards.

#### Advancements in Predictive Modeling

---

Traditional regression models initially formed the basis for predicting retro-reflectivity degradation. (Swargam, 2004) reported low predictive accuracy for these models ( $R^2$  values ranging from 9.99% to 33.52%), while subsequent efforts by (Rasdorf et al., 2006) and (Immaneni et al., 2009) improved this range to 20%–52%. These studies reaffirmed age as a dominant predictor and estimated retro-reflectivity minimums to be reached 8–15 years post-installation. However, these models struggled to capture non-linear relationships between factors.

Machine learning techniques have since transformed predictive modeling. Neural networks demonstrated  $R^2$  values of 97.6%, significantly outperforming polynomial regression (75.9%) (Saleh & Fleyeh, 2024b). Random Forest and Support Vector Machines further enhanced prediction accuracy, achieving F1 scores of 98% in 2022. These advancements highlight the ability of machine learning models to handle complex interactions among variables, making them more suitable for predicting retro-reflectivity degradation.

#### Comparative Performance of Models

---

The superiority of machine learning models is evident when comparing their performance to traditional methods. (Jamal et al., 2022b) evaluated Feed-Forward, Cascade Forward, and Elman Neural Networks using data from 539 traffic signs in Pakistan, finding that the Elman Neural Network demonstrated the highest predictive accuracy. (Similarly, (Alkhulaifi et al., 2021) employed deep learning models that integrated diverse inputs, including sheeting brand, grades, colors, and observation angles, achieving superior results compared to regression methods. Huang et al. (2013) also found that quadratic and cubic regression models outperformed linear models for predicting retro-reflectivity degradation across different sheeting types. These findings underscore

the need for sophisticated, data-driven approaches to improve retro-reflectivity predictions.

Despite substantial research on retro-reflectivity prediction, critical gaps remain, particularly in the application of computer vision models and the incorporation of environmental factors, such as air temperature, humidity, and pollution. This study addresses these gaps by leveraging deep learning and computer vision techniques to develop a robust predictive framework. By integrating environmental variables with diverse sign attributes, including age and shading conditions, it curates a combined image and tabular retro-reflectivity dataset to enhance prediction accuracy and overcome data limitations. The resulting model will forecast retro-reflectivity values, classify signs as compliant or non-compliant, and support efficient maintenance planning, ensuring road safety and adherence to MUTCD standards.

### Challenges and Gaps

---

Existing research has extensively examined the prediction of retro-reflectivity and its influencing factors, such as the age and physical properties of traffic signs. However, the integration of computer vision models with environmental variables for estimating retro-reflectivity remains unexplored. Alkhulaifi et al., 2021 developed a deep learning model that identified key predictors and outperformed earlier methods but did not incorporate image datasets into its framework. This gap highlights the opportunity to leverage deep learning and computer vision to estimate retro-reflectivity more comprehensively and analyze the influence of environmental factors, such as air temperature and humidity. Despite this potential, several critical challenges must be addressed to achieve accurate and reliable predictions as outlined below:

- Lack of a corresponding image dataset to complement the existing tabular retro-reflectivity data limits the data scope necessary for accurate predictive classification.
- Retro-reflectivity degradation is highly sensitive to factors like air temperature and humidity, introducing variability that complicates predictive model accuracy.
- Existing studies have not incorporated sign retro-reflectivity deterioration across different sign attributes and aging conditions into a single model, limiting the scope and generalizability of current predictions.

## CHAPTER 3

### Method

This section presents a systematic approach to predicting retro-reflectivity degradation in traffic signs, integrating advanced data collection, qualitative analysis, and predictive modeling as shown in Figure 1. It begins by describing the study area and detailing the data collection process, including the acquisition of image and tabular datasets essential for modeling retro-reflectivity. A qualitative analysis follows, identifying key patterns influencing retro-reflectivity. Finally, retro-reflectivity degradation prediction models are developed using state-of-the-art machine learning techniques to address identified challenges and enhance prediction accuracy.

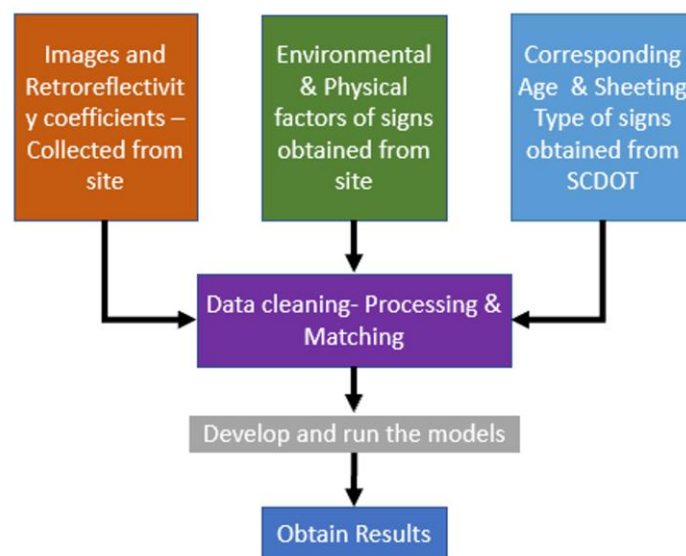


**Figure 1 Workflow diagram showing the integration of retro-reflectivity coefficients, environmental factors, and sign attributes into a dataset, followed by data cleaning, model development, and retro-reflectivity prediction.**

#### Study area and Data collection.

##### a) Study area

The traffic sign data was collected in Orangeburg County, South Carolina, USA, using a calibrated RetroSign retroreflectometer to measure retroreflectivity (RA in  $\text{cd/lx/m}^2$ ). During the data collection process, we recorded various attributes, including sign images, height, GPS location, temperature, and humidity. In total, 586 traffic signs were documented before any pre-processing. Signs with missing data were removed from the dataset prior to analysis.

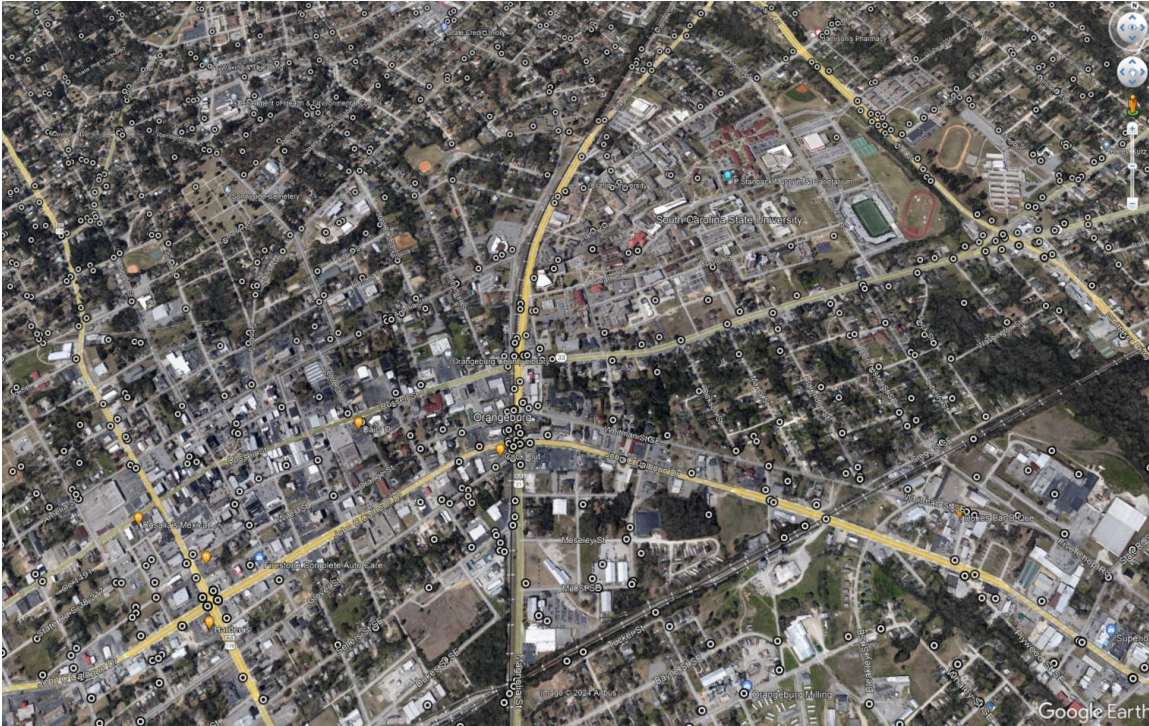


**Figure 2 Traffic signs in Orangeburg County, South Carolina, documented as part of the study and obtained from the South Carolina Department of Transportation (SCDOT).**

**b) Data Collection.**

The data collection process employed the RetroSign GRX 1 retroreflectometer to capture images of traffic signs and record key attributes. These attributes included the background color, legend color, coefficient of retroreflected luminance (RA in  $\text{cd/lx/m}^2$ ), contrast, GPS coordinates (latitude and longitude), temperature, and relative humidity.

The RetroSign GRX 554 retroreflectometer, as shown in the Figure 3 , was the primary instrument used to measure the coefficient of retroreflectivity for all traffic signs in this study. This handheld device is specifically designed for measuring the retroreflectivity of road signs, conspicuity tape, license plates, and safety clothing. It supports models with 1, 3, or 7 observation angles and complies with international standards, including EN 12899, EN 20471, ASTM E 1709, and ASTM E 2540. Key features of the RetroSign include fast calibration, automatic averaging, pass/fail checks, and advanced data processing capabilities. Additional functionalities, such as a built-in camera enabling sign image data collection, GPS, barcode/QR code reader, and wireless communication, enhance its utility for field studies.



**Figure 3 The handheld RetroSign GRX 554 retroreflectometer, used for measuring traffic sign retro-reflectivity during the study (TAPCO, 2024).**

An important step in using the retroreflectometer is calibrating it to ensure accurate and consistent readings that meet regulatory requirements for reliable retro-reflectivity measurements. Before each use, the device is calibrated with a certified reference panel that contains known reflective calibration values, as illustrated in Figure 4.

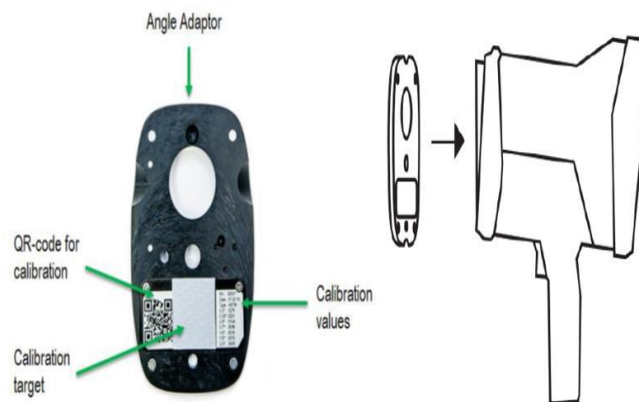


**Figure 4 Calibration of the RetroSign GRX 554 retroreflectometer, demonstrating the attachment of the calibration standard and preparation for accurate retro-reflectivity measurements.**

The calibration process began by cleaning the instrument's optics and the calibration panel to remove any dust or debris that could interfere with the readings. The calibration standard is then attached to the designated calibration side, while the front plate is secured to the measuring side. Once everything is set to the correct angle and distance from the panel, the retroreflectometer performs a series of automated readings after the "capture" button is pressed. These readings are compared to the reference values, and adjustments are made as necessary to ensure the device is within specification. This rigorous calibration process guarantees that the RetroSign GRX 554 provides reliable data for maintaining the visibility and safety of traffic signs.

After calibration, the retroreflectometer was positioned perpendicular to the surface of the traffic sign to take measurements. To ensure consistency, four readings were recorded for each color of the sign, including both the background and the legend, as shown in Figure 5.



**Figure 5 Shows measuring and recording the retroreflectivity coefficient of the Legend color of a stop sign in the study area**

The coefficient of retroreflected luminance (RA in  $\text{cd/lx/m}^2$ ) for each observation, along with background color, legend color, contrast, GPS coordinates (latitude and longitude), temperature, and relative humidity, were automatically recorded in the retroreflectometer. Some of the collected images are presented in Figure 6.



**Figure 6 Some of the Images of road signs collected using a retro-reflectometer in the study area.**

The height of the sign from the ground was also, measured using a tape measure and recorded in inches. Similarly, the signs in shades and directly exposed to the sun were recorded, i.e. (shading condition).

We collected Images of 586 signs with their corresponding attributes which are the Legend Ra  $0.2^\circ$ , Background Ra  $0.2^\circ$ , Latitude ( $^\circ$ ), Longitude ( $^\circ$ ), Temperature ( $^\circ\text{C}$ ), Rel. Humidity (%), Height (inches), Shading condition (Yes/No). ) Additional data, that included the age and sheeting type of the signs, were obtained from the South Carolina Department of Transportation (SCDOT).

## Qualitative Analysis of the Data

### A) Traffic signs image and tabular data analysis

Data preprocessing began by matching the collected field data with the information available in the South Carolina Department of Transportation database. Signs with indeterminate ages were excluded, resulting in a total of 188 signs used for the analysis.

### B) Correlation Analysis

We conducted a correlation analysis to understand and quantify the strength and direction of relationships between variables during the initial stages of data preprocessing. This step was crucial for preparing data for classification and regression models. By considering related variables, we aimed to improve model accuracy by ensuring predictions were based on relevant and unique information. The heatmap is shown in Figure 7, we illustrate the correlation coefficients within the collected data. We observed three pairs of variables with significant positive correlations: (Legend color and Legend Ra), (Legend color and Contrast), and (Legend Ra and Contrast). Additionally, two pairs of variables exhibited significant negative correlations: (Background color and Contrast) and (Background Ra and Contrast). These correlations align with the uniform color patterns present in the dataset.

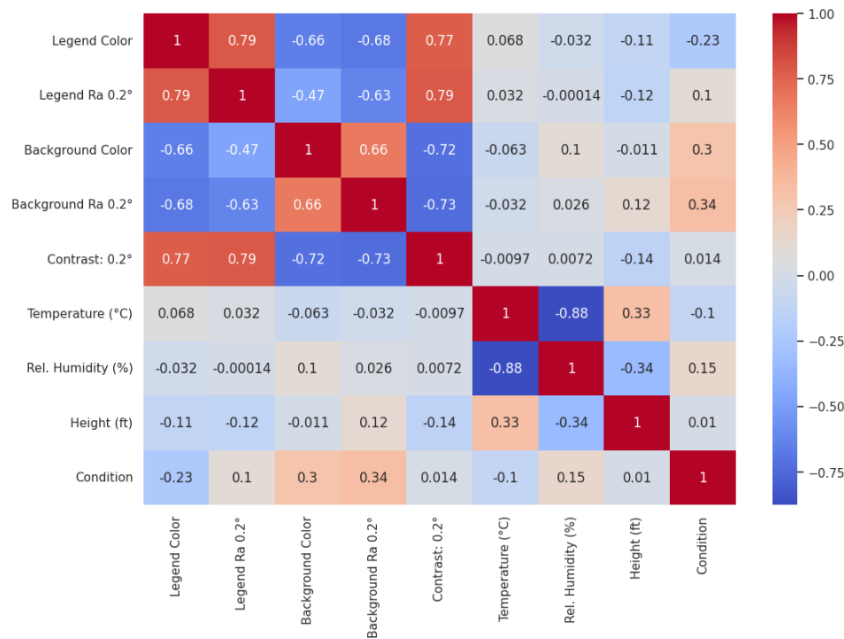


Figure 7 Correlation analysis in collected data

## Retro-Reflection Degradation Prediction Models

### a) XGBoost for Traffic Sign Classification

XGBoost was employed for the classification task to predict the condition of traffic signs based on their retroreflectivity values. This supervised learning algorithm uses training data  $x_i$  with multiple features to predict a target variable  $y_i$ . For this study, two classes were defined: traffic signs meeting the minimum retroreflective values stipulated by the MUTCD were classified as "good," while those falling below the threshold were classified as "bad." The flexibility and efficiency of XGBoost make it ideal for handling such classification tasks, especially with large datasets containing complex feature interactions. As an efficient implementation of the gradient boosting algorithm, XGBoost combines multiple weak learners (decision trees) to form a strong predictive model. The algorithm iteratively builds an ensemble of trees to minimize a regularized objective function:

$$\mathcal{L}(\theta) = \sum_{i=1}^n l(y_i, \hat{y}_i) + \sum_{k=1}^K \Omega(f_k),$$

where  $l(y_i, \hat{y}_i)$  is the loss function and  $\Omega(f_k)$  penalizes model complexity. At each iteration, the model fits a new tree to correct residuals and update predictions:

$$\hat{y}_i^{(t)} = \hat{y}_i^{(t-1)} + f_t(x_i),$$

To achieve precise optimization, XGBoost leverages first-order gradients  $g_i$  and second-order Hessians  $h_i$ , which account for both the magnitude and curvature of the loss function. The regularization term further helps control overfitting:

$$\Omega(f_k) = \gamma T + \frac{1}{2} \lambda \|w\|^2,$$

These features, along with parallel computation and the ability to handle missing data, make XGBoost highly scalable and effective. Its robust optimization framework ensures reliable classification of traffic signs into "good" or "bad" conditions, supporting informed decisions for retroreflectivity maintenance.

### b) EfficientNet-B0 for the Regression Task

We developed a fusion regression model to predict traffic sign retroreflectivity values using images and corresponding tabular data. For the image regression task, we employed a Convolutional Neural Network (CNN) based on the EfficientNet-B0 architecture. EfficientNet-B0 belongs to a family of CNNs that exhibit efficiency and strong performance in computer vision tasks. We designed it using a combination of manual design and neural architecture search (NAS) while incorporating a novel compound scaling technique. This technique balances depth, width, and resolution for efficiency and can be expressed as:

$$d = \alpha^k, w = \beta^k, r = \gamma^k$$

where  $d$ ,  $w$ , and  $r$  represent depth, width, and resolution, respectively, while  $\alpha$ ,  $\beta$ , and  $\gamma$  are scaling factors determined through NAS. By uniformly scaling these dimensions, we ensured that EfficientNet-B0 achieved a balance between accuracy and computational efficiency.

EfficientNet-B0's architecture consists of a stem, repeated blocks, and a head, incorporating depth wise separable convolutions, squeezed bottlenecks, and pointwise convolutions.

The MBConv block, central to its structure, is defined as:

$$MBConv(x) = PW(DW(x) \odot SE(DW(X)))$$

where  $x$  represents the input feature map,  $DW(\cdot)$  performs depthwise convolutions,  $PW(\cdot)$  applies pointwise convolutions, and  $SE(\cdot)$  adjusts channel weights using squeeze-and-excitation. These components collectively reduce computational costs while preserving model accuracy, making EfficientNet-B0 particularly suited for image regression tasks where computational efficiency is critical.

We minimized the regression objective using the Mean Squared Error (MSE) loss, defined as:

$$\mathcal{L}_{MSE} = \frac{1}{n} \sum_{i=1}^r (y_i - \hat{y}_i)^2$$

where  $y_i$  is the true retroreflectivity value,  $\hat{y}_i$  is the predicted retroreflectivity value, and  $n$  is the number of samples. We employed transfer learning to leverage pre-trained weights, reduce training time, enhance feature extraction, and mitigate overfitting. We chose EfficientNet-B0 for its computational efficiency and strong feature representation capabilities, making it an ideal choice for this task.

## CHAPTER 4

### Experimental Setup

#### Experimental Setup

The dataset used for the experiments, described in Chapter 3, was split into 80% training and 20% testing sets. The tabular training set comprised 151 records, while the testing set included 37 records. Similarly, the image training set contained 151 records, and the image testing set included 37 records, both used for model evaluation.

For the classification task, image data was processed using an Extreme Gradient Boosting (XGBoost) model to classify traffic signs as "good" or "bad" based on retroreflectivity levels. Signs meeting the MUTCD's minimum retroreflective values were labeled as "good," while those below the threshold were labeled as "bad." Data preprocessing in Python included normalization, encoding of categorical variables, and defining target labels based on retroreflectivity conditions. For the regression task, a multi-regression model was implemented to predict retroreflectivity values using both tabular and image data. Data preprocessing in Python included normalization and encoding of categorical variables.

All models, including those for classification and regression, were trained using an NVIDIA – SMI A100 – SXM4-40GBGPU on Google Colab+, ensuring computational efficiency.

#### Hyper-parameter Tuning

The hyper-parameters of the XGBoost classifier used to build the classification model are summarized in Table 1.

**Table 1: XGBoost Hyper-parameter Settings.**

Hyper-parameter	Values
learning_rate	0.01
eta	0.075
n_jobs	-1
max_depth	90
n_estimators	1000
min_child_weight	5
subsample	1.0
colsample_bytree	1.0

## Evaluation Metrics

The model's classification performance is assessed using the weighted average values of precision, recall, and F1-score, as specified in Eq. 4 through Eq. 6. are adopted as the metrics to evaluate the performance of the classification model. These metrics are calculated based on the true positives ( $tp_i$ ), true negatives ( $tn_i$ ), false positives ( $fp_i$ ), and false negatives ( $fn_i$ ) for each defect class  $C_i$ , where  $i$  ranges from 1 to  $m$  and  $m$  denotes the total number of defect classes in the dataset. Here,  $|Y_i|$  represents the number of samples assigned to each defect class.

$$\text{Weighted Average Precision} = \frac{\sum_{i=1}^m |Y_i| \frac{tp_i}{tp_i + fp_i}}{\sum_{i=1}^m |Y_i|}$$

$$\text{Weighted Average Recall} = \frac{\sum_{i=1}^m |Y_i| \frac{tp_i}{tp_i + fn_i}}{\sum_{i=1}^m |Y_i|}$$

$$\text{Weighted Average F1 - score} = \frac{\sum_{i=1}^m |y_i| \frac{2tp_i}{2tp_i + fp_i + fn_i}}{\sum_{i=1}^m |y_i|}$$

We also evaluated the performance of our regression model using Mean Squared Error (MSE), Mean Absolute Error (MAE), and the Coefficient of Determination (R2), as defined in Eq. 7 through Eq. 9. These metrics allowed us to quantify the accuracy and reliability of the predicted retroreflectivity values compared to the actual values ( $y_i$ ) across  $n$  samples in the dataset.

We used MSE to measure the average squared difference between actual and predicted values, emphasizing larger errors:

$$MSE = \frac{1}{n} \sum_{i=1}^n (y_i - \hat{y}_i)^2$$

To assess the average magnitude of errors regardless of direction, we used MAE, which provides a more interpretable measure:

$$MAE = \frac{1}{n} \sum_{i=1}^n |y_i - \hat{y}_i|$$

We also calculated R2, the Coefficient of Determination, to evaluate how well our model explained the variance in actual values. Higher R2 values, closer to 1, indicated better performance:

$$R^2 = 1 - \frac{\sum_{i=1}^n (y_i - \hat{y}_i)^2}{\sum_{i=1}^n (y_i - \bar{y})^2}$$

Here,  $\bar{y}$  represents the mean of the actual values. By combining these metrics, we obtained a comprehensive understanding of our model's predictive capability, balancing sensitivity to large errors (MSE), overall accuracy (MAE), and explained variance ( $R^2$ ).

## CHAPTER 5

### Results and Discussion

#### Results and Discussion

---

##### A. Predicting the Condition of Traffic Signs Based on retroreflectivity Levels

The classification model achieved an overall accuracy of 0.97, correctly predicting 97% of instances. Performance differed significantly between the two classes. For Class 0 (bad condition), the model recorded a precision and recall of 0.00, indicating no positive instances of this class were correctly identified. In contrast, for Class 1 (good condition), the model achieved a precision of 0.97, a recall of 1.00, and an F1-score of 0.98. Support values confirmed an imbalance in the dataset, with only 4 instances for Class 0 compared to 127 for Class 1. The macro average precision, recall, and F1-score were 0.48, 0.50, and 0.49, respectively, reflecting equal weighting across classes. The weighted average, which accounts for class distribution, showed precision, recall, and F1-score of 0.94, 0.97, and 0.96, respectively. These results highlight the model's strong overall performance, particularly for Class 1.

##### B. Predicting Retroreflectivity Values Using Transfer Learning with EfficientNet-B0

The EfficientNet-B0 model, applied for image regression, achieved a test Mean Absolute Error (MAE) of 57.562 and a test loss of 6783.265, with an R2 value of 0.791. These results demonstrate that the model successfully extracted features from the images to predict retroreflectivity values with reasonable accuracy. The R2 value indicates that approximately 71.1% of the variance in retroreflectivity values is explained by the model, reflecting its effectiveness. The achieved MAE highlights the model's ability to provide meaningful predictions, validating the potential of transfer learning with EfficientNet-B0 for this task.

The model achieved a test Mean Absolute Error (MAE) of 57.562 and a test loss of 6783.265 with an R2 of 0.791. These results show that the model captures features from the images to make predictions of the retroreflectivity.

## CHAPTER 6

### Conclusion and Future Work

#### Conclusion and Future Work

---

In this study, we applied deep-learning models to predict the retroreflectivity of road traffic signs using image detection techniques. We considered factors influencing retroreflective degradation, such as weather conditions, air pollution, air temperature, and relative humidity. Our transfer learning model, EfficientNet-B0, achieved a test Mean Absolute Error (MAE) of 57.562, a test loss of 6783.265, and an R2 value of 0.791, effectively predicting retroreflectivity values. These results demonstrate the potential of deep-learning techniques to estimate traffic sign retroreflectivity, offering promising applications for reducing maintenance costs and

improving road safety by minimizing risks for maintenance crews.

In future work, we aim to address the observed class imbalance in our dataset, which limits the model's ability to generalize to under-represented conditions. We plan to expand data collection to include diverse geographic regions, environmental conditions, and a wider range of retroreflectivity states to mitigate this imbalance. Additionally, we will explore class balancing techniques, such as oversampling and advanced algorithms, to improve prediction accuracy

for under-represented categories. Furthermore, we intend to incorporate additional influencing factors, such as UV radiation exposure and traffic density, and to leverage multi-modal data, including video and tabular inputs, to enhance model performance. These efforts will support the development of more robust and reliable systems for traffic sign maintenance and management.

## REFERENCES

- Alkhulaifi, A., Jamal, A., & Ahmad, I. (2021). Predicting Traffic Sign Retro-Reflectivity Degradation Using Deep Neural Networks. *Applied Sciences*, 11(24), 11595. <https://doi.org/10.3390/app112411595>
- Ansari, S., Naghdy, F., & Du, H. (2022). Human-Machine Shared Driving: Challenges and Future Directions. *IEEE Transactions on Intelligent Vehicles*, 7(3), 499–519. <https://doi.org/10.1109/TIV.2022.3154426>
- Brimley, B., Mousavi, S. M., Carlson, P., & Dixon, K. (2017, January). *Safety Effects of Traffic Sign Upgrades in Albuquerque, New Mexico*.
- Huang, W., Hu, L., & Jiang, M. (2013). Retroreflectivity and Deterioration Characteristics of Sheeting Used for In-Service Guide Signs. *Journal of Highway and Transportation Research and Development (English Edition)*, 7(2), 88–93. <https://doi.org/10.1061/JHTRCQ.0000320>
- Immaneni, V. P., Hummer, J. E., Rasdorf, W. J., Harris, E. A., & Yeom, C. (2009). *Synthesis of sign deterioration rates across the United States*. *J. Transp. Eng.* 135 (3), 94–103.
- Jamal, A., Reza, I., & Shafiullah, M. (2022a). Modeling retroreflectivity degradation of traffic signs using artificial neural networks. *IATSS Research*, 46(4), 499–514. <https://doi.org/10.1016/j.iatssr.2022.08.003>
- Jamal, A., Reza, I., & Shafiullah, M. (2022b). Modeling retroreflectivity degradation of traffic signs using artificial neural networks. *IATSS Research*, 46(4), 499–514. <https://doi.org/10.1016/j.iatssr.2022.08.003>
- Khalilikhah, M., & Heaslip, K. (2016). The effects of damage on sign visibility: An assist in traffic sign replacement. *Journal of Traffic and Transportation Engineering (English Edition)*, 3(6), 571–581. <https://doi.org/10.1016/j.jtte.2016.03.009>
- Rasdorf, W. J., Hummer, J. E., Harris, E. A., Immaneni, V. P. K., & Yeom, C. (2006). Designing an efficient nighttime sign inspection procedure to ensure motorist safety (No. FHWA/NC/2006-08). . *North Carolina Department of Transportation, Research and Analysis Group*.
- Roxan Saleh. (2021). *Analysis of Retroreflection and other Properties of Road Signs*.
- Saleh, R., & Fleyeh, H. (2021). Factors Affecting Night-Time Visibility of Retroreflective Road Traffic Signs : A Review. *International Journal for Traffic and Transport Engineering*, 11(1), 115–128. [https://doi.org/10.7708/ijtte.2021.11\(1\).07](https://doi.org/10.7708/ijtte.2021.11(1).07)
- Saleh, R., & Fleyeh, H. (2024a). Predictive models for road traffic sign: Retroreflectivity status, retroreflectivity coefficient, and lifespan. *International Journal of Transportation Science and Technology*. <https://doi.org/10.1016/j.ijst.2024.02.008>
- Saleh, R., & Fleyeh, H. (2024b). Predictive models for road traffic sign: Retroreflectivity status, retroreflectivity coefficient, and lifespan. *International Journal of Transportation Science and Technology*. <https://doi.org/10.1016/j.ijst.2024.02.008>
- Swargam, N. (2004). *Development of a neural network approach for the assessment of the performance of traffic sign retroreflectivity*.
- Wolshon, B., Swargam, J., & Degeyter, R. (2022). *ANALYSIS AND PREDICTIVE MODELING OF ROAD SIGN RETROREFLECTIVITY PERFORMANCE*.